

Vinyl Ethylene Carbonate as an Effective SEI-Forming Additive in Carbonate-Based Electrolyte for Lithium-Metal Anodes

Yang Yang,[†] Jian Xiong,[‡] Shaobo Lai,[‡] Rong Zhou,[‡] Min Zhao,[‡] Hongbo Geng,[†] Yufei Zhang,[†] Yanxiong Fang,[†] Chengchao Li,^{*,†,§} and Jinbao Zhao^{*,†,§}

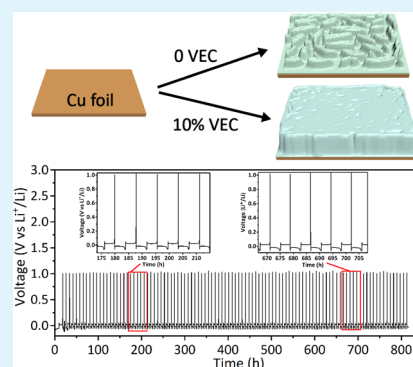
[†]School of Chemical Engineering and Light Industry, Guangdong University of Technology, Guangzhou 510006, China

[‡]State Key Laboratory of Physical Chemistry of Solid Surfaces, College of Chemistry and Chemical Engineering, Collaborative Innovation Center of Chemistry for Energy Materials, Xiamen University, Xiamen 361005, China

Supporting Information

ABSTRACT: We report the use of vinyl ethylene carbonate as a new solid electrolyte interface (SEI)-forming additive for Li-metal anodes in carbonate-based electrolyte, which has the advantages of both good storage performance and low price. Compared to the SEI formed in vinyl ethylene carbonate-free electrolyte, the SEI film formed in 10% vinyl ethylene carbonate electrolyte contains a higher relative content of polycarbonate species and a greater amount of decomposition products of LiPF₆ salt. Both components are expected to have positive effects on the passivation of Li-metal surface and the accommodation of volume changes of anode during cycling. Scanning electron microscopy images and COMSOL numerical simulation results further confirm that uniform Li deposition morphology can be achieved in the presence of vinyl ethylene carbonate additive. When cycling at the current density of 0.25 mA cm⁻² with a cycling capacity of 1.0 mAh cm⁻², the vinyl ethylene carbonate-contained Li–Cu cell exhibits a long life span of 816 h (100 cycles) and a relatively high Coulombic efficiency of 93.2%.

KEYWORDS: lithium-ion battery, Li-metal anode, vinyl ethylene carbonate, SEI, electrolyte additive, numerical simulation



1. INTRODUCTION

With the rapid development of grid energy storage and electric vehicles, developing rechargeable battery with high energy density and power capability is extremely urgent.¹ Among numerous rechargeable batteries, lithium-ion battery is regarded as a powerful electrochemical energy-storage device and has been applied to various portable devices widely.^{2,3} Although commercial graphite-based anode materials have approached their theoretical limit, they can still hardly meet the urgent need of high energy density applications.⁴ Among these anode candidates, lithium-metal anode has attracted special attention due to its super theoretical specific capacity (3860 mAh g⁻¹) and the most negative reduction electrochemical potential (−3.045 V vs standard hydrogen electrode).⁵ Many researchers believe that the successful application of Li-metal anode will lead to a huge revolution in the energy-storage field.

Although early in the 1980s Whittingham et al. had attempted to use Li metal as anode and TiS₂ as cathode to fabricate a secondary Li battery, the uncontrolled growth of Li dendrites had prevented its commercialization.^{6–8} To date, the obstacles that hinder the practical application of Li-metal anodes are as follows: (1) huge volume changes during Li plating/stripping owing to the natural hostless deposition mechanism can cause cracks of solid electrolyte interface (SEI) films, and the low impedance and enhanced ion flux in the cracked regions will aggravate the nonuniform deposition

behavior and accelerate the appearance of dendritic Li; (2) the continuous growth of Li dendrites may pierce through polymeric separator and contact with cathode, leading to the short circuit of batteries; and (3) the repeated crack and repair of SEI films will give rise to low Coulombic efficiency (CE) and poor cycle life upon cycling.

Thus, building a stable, robust, and protective SEI layer on the interface of Li-metal anodes is one of the most effective methods to restrain the growth of Li dendrites and reduce side reactions between highly reactive fresh-deposited Li and electrolyte. Extensive efforts have been made to obtain improved SEI. Introducing artificial SEI films such as Li-conducting Li₃PO₄ layer,⁹ soft and highly viscoelastic polymer coating layer,¹⁰ poly(dimethylsiloxane) thin film,¹¹ poly(ethyl α -cyanoacrylate)-based interphase layer,¹² LiF coating layer,¹³ poly(vinylidene-co-hexafluoropropylene), and LiF hybrid film¹⁴ has been proved to be a good modification method for offering good mechanical strength and shape conformability to restrain the formation of Li dendrites. However, there is a key disadvantage that these artificial SEI layers generally should be synthesized and coated onto Li-metal anodes in advance.

Received: November 25, 2018

Accepted: January 17, 2019

Published: January 17, 2019

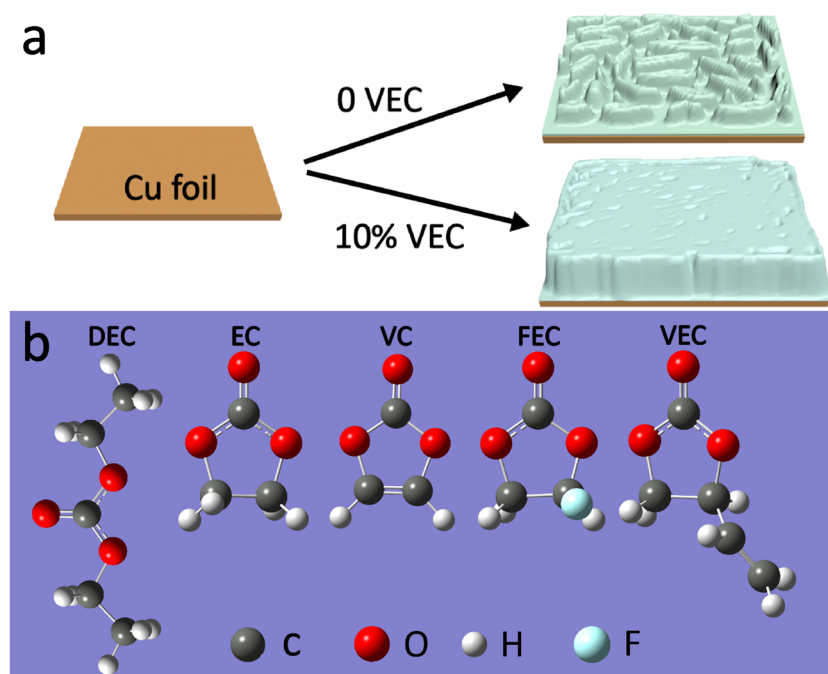


Figure 1. (a) Illustration of the SEI-forming function of VEC additives on the surface of Li-metal anode. (b) Structural formulae of diethylene carbonate (DEC), EC, VC, FEC, and VEC.

On the other hand, adding appropriate additives into the electrolyte can also contribute to an improved SEI, which is formed in situ during cycling.^{15–17} Compared with fabricating the ex situ artificial SEI, this in situ approach is facile and cheap, particularly suitable for industrial manufacture of batteries.^{18,19} LiNO_3 , KNO_3 , and polysulfides as additives can improve the cycle life and CE in ether-based electrolyte.^{20–22} But the intrinsic relatively narrow voltage windows of ether-based electrolytes (generally used 1,3-dioxolane/dimethyl ether solution is only chemically stable to ~ 3.58 V) may impede the utilization of Li-metal batteries when matching with high-voltage cathodes.²³ The antioxidation capability of carbonate-based electrolytes is obviously better, in which vinylene carbonate (VC) and fluoroethylene carbonate (FEC) are highly considered as effective additives by regulating organic and inorganic constituents in the SEI film.^{24–26} However, VC is an unstable compound even at room temperature because it tends to be polymerized into poly(vinyl carbonate).^{27,28} Although FEC is more stable, its high price (USD 545/25 g, Sigma-Aldrich) inspires researchers to find an alternative of FEC.

Vinyl ethylene carbonate (VEC) is a commonly used electrolyte additive for graphite anodes.^{28–31} But to the best of our knowledge, there are few studies about the impact of VEC on Li-metal anodes. Herein, the effect of VEC (USD 56.6/25 g, Sigma-Aldrich) as a highly effective and low-cost SEI-forming additive for Li-metal anodes in carbonate-based electrolyte was explored (Figure 1a). The molecular structure of VEC is similar to that of VC, composed of carbon double bonds and ring molecular structure (Figure 1b). But the storage performance of VEC is much better than that of VC, on account of the slightly electron-rich double bond of VEC, and therefore the reactivity with other double bonds is lower.^{28,32} The function of VEC additive for Li-metal anodes is verified by the Li|Cu half-cell tests and COMSOL numerical simulation. The formation of a dense and uniform SEI on Li-metal anode is confirmed. Therefore, enhanced CE and cycling life can be

achieved in the presence of VEC additive in carbonate-based electrolyte.

2. EXPERIMENTAL SECTION

2.1. Materials. The electrolyte of 1.0 M lithium hexafluorophosphate (LiPF_6) in 1:1 v/v ethylene carbonate (EC, > 99.9%) and diethylene carbonate (DEC, > 99.9%) was received from Zhangjiagang Guotai-Huarong New Chemical Materials Co., Ltd. The VEC additive (99%) was purchased from Alfa Aesar. All reagents were used as received.

2.2. Characterization. For the need of measurements, the Li-deposited electrodes were disassembled from the coin cells, rinsed three times with dimethyl carbonate, and dried in an Ar-filled glovebox. The morphologies of the electrodes were characterized by scanning electron microscope (S-4800, Hitachi). Fourier transform infrared (FTIR) spectra were performed on an FTIR spectrometer (Nicolet ISS, Thermo Scientific). X-ray photoelectron spectroscopy (XPS) measurements were conducted on an X-ray scanning microprobe electron energy spectrometer (Quantum 2000, Physical Electronics).

2.3. Density Functional Theory (DFT) Calculation. The quantum chemical calculations of highest occupied molecular orbital (HOMO) and lowest unoccupied molecular orbital (LUMO) energy levels were executed by Gaussian 09 package. The B3PW91 functional and 6-311+G(d,p) basis sets were used to optimize the structures.³³

2.4. Electrochemical Measurement. The CR 2016-type coin cells were assembled in an Ar-filled glovebox with the contents of both O_2 and H_2O below 1.0 ppm. Cu foil was used as the working electrode. Li-metal foil with diameter of 12 mm and thickness of 1 mm was used as the counter electrode. The Celgard 2400 membrane was used as the separator, and the solution of 1 M LiPF_6 in EC/DEC (v/v = 1:1) with and without 10% VEC was used as the electrolyte. For all of the batteries, a fixed amount of Li (1.0 mAh cm^{-2}) was deposited onto the Cu foil and then stripped away up to 1.0 V at a relatively low current density of 0.1 mA cm^{-2} in the initial cycle to stabilize the SEI. For the subsequent cycles, different current densities (0.25 , 0.5 , or 1.0 mA cm^{-2}) were employed. Electrochemical impedance spectroscopy (EIS) was measured by using the Autolab Potentiostat Galvanostat 302 N from 10 mHz to 100 kHz. All of the electrochemical measurements were taken at room temperature.

Table 1. Calculated Values of the HOMO and LUMO Energy Levels of Solvents (EC and DEC) and Additives (FEC, VC, and VEC) at the B3PW91 Functional and 6-311+G(d,p) Level of Theory

		HOMO (eV)	LUMO (eV)
solvent	EC	-8.73	0.02
	DEC	-8.38	0.03
additive	FEC	-9.10	-0.03
	VC	-7.30	-0.25
	VEC	-7.98	-0.82

3. RESULTS AND DISCUSSION

Figure 1b and Table 1 show the molecular structure and HOMO and LUMO energy levels of EC, DEC, FEC, VC, and VEC. A semiempirical rule is that the lower value of LUMO energy level will lead to lower resistance toward the reduction of molecule, meaning the reduction reaction may start at a higher potential. And it is generally accepted that the formation of SEI starting at a higher potential will lead to a denser film.¹⁹ As shown in Table 1, the order of values of LUMO energy level is VEC < VC < FEC < EC < DEC. The calculation results reveal that VEC may be reduced prior to both the additives of FEC and VC and the solvents of EC and DEC during the initial Li plating process. Although the reduction activity of VEC is relatively higher, the addition of VEC does not affect the long-term stability of electrolyte against the highly reductive environment (Figure S1).

For exploring the differences of chemical makeup between the SEI films formed in VEC-containing and VEC-free electrolytes, FTIR and XPS measurements were performed. For the SEI film formed in 0% VEC electrolyte, the two small peaks located at 1804 and 1774 cm^{-1} are characteristic peaks of polycarbonate species (ROCO_2R) related to $\text{C}=\text{O}$ stretching (Figure 2).^{26,32} The pronounced peaks at 1638, 1313, 1195,

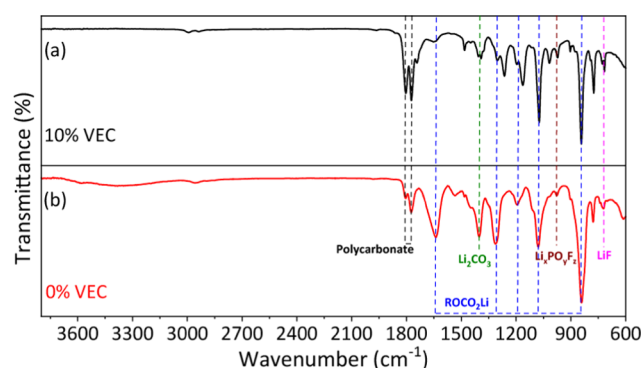


Figure 2. Comparison of FTIR spectra of SEI films formed on the Cu foil electrodes after 10 cycles at 0.25 mA cm^{-2} for 1.0 mAh cm^{-2} in different electrolytes: (a) 1 M LiPF_6 in EC/DEC (1:1 by volume) with 10% VEC and (b) 1 M LiPF_6 in EC/DEC (1:1 by volume) without VEC.

1079, and 841 cm^{-1} are ascribed to ROCO_2Li , which is one of the main reduction products of EC on Li electrodes.^{34,35} The band present around 1402 cm^{-1} is the typical peak of Li_2CO_3 .³⁶ And two weak peaks at 977 and 721 cm^{-1} should be attributed to $\text{Li}_x\text{PO}_y\text{F}_z$ and LiF, respectively (decomposition products of LiPF_6 salt).^{37,38} In the case of 10% VEC electrolyte, peaks of polycarbonate species, ROCO_2Li , Li_2CO_3 , $\text{Li}_x\text{PO}_y\text{F}_z$, and LiF can also be found. Moreover, it can be

clearly seen that the polycarbonate species in the SEI film of 10% VEC is obviously richer than that in 0% VEC. According to the research works of the Aurbach group, polycarbonate species in the SEI layer are more cohesive and flexible than ROCO_2Li , which are expected to have positive effects on the passivation of Li-metal surface and the accommodation of volume changes of anode during repeated cycling.^{34,39}

Figure 3 presents XPS patterns of SEI films on Cu foil electrodes formed in the two electrolyte solutions. The corresponding element contents estimated from XPS survey spectra are also shown in the inset image. C and F elements in the SEI film of 10% VEC are obviously richer than those in VEC-free electrolyte (Figure 3a). For the high-resolution C 1s spectra (Figure 3b,d), XPS images exhibit three peaks located at 284.8 eV (nonoxygenated C–, C–C–, and C–H-containing species), 286.2 eV (C–O band), and 289.9 eV (OC(=O)O band).⁴⁰ The relative intensity ratio of nonoxygenated C/oxygenated C band of SEI layer in 10% VEC electrolyte (1.10) is higher than that in 0% VEC electrolyte (0.77). This is because the SEI film of 10% VEC contains a higher proportion of polycarbonate species, and the relative content of C/O element of long-chain polycarbonate species is much higher than that of ROCO_2Li . Possible reduction mechanisms of DEC, EC, and VEC are listed in Figure S2. For the high-resolution F 1s spectra (Figure 3c,e), both XPS image should be deconvoluted into two peaks of $\sim 685.3 \text{ eV}$ (LiF) and $\sim 687.1 \text{ eV}$ ($\text{Li}_x\text{PO}_y\text{F}_z$). The relative intensity of LiF/ $\text{Li}_x\text{PO}_y\text{F}_z$ in 10% VEC electrolyte (0.87) is much higher than that in 0% VEC electrolyte (0.28). And LiF is widely considered to play a very important role in the formation of uniform and stable SEI to suppress the growth of Li dendrites.^{13,25,41} More LiF on the interface of Li-metal anode is beneficial to the passivation of electrode surface and the suppression of electron leakage. And on the other hand, stable Li electrodeposition process can be achieved by enhancing interfacial transport of Li^+ ions.^{42,43} XPS patterns of SEI films formed on the Cu foil electrodes after 25 cycles at 0.25 mA cm^{-2} for 1.0 mAh cm^{-2} in 10% VEC electrolyte were also investigated (Figure S3).

Combining the information provided by FTIR and XPS images, the distinctive features of the SEI film formed on Li-metal anodes in 10% VEC electrolyte compared to those in 0% VEC electrolyte are as follows:

- (1) The SEI film formed in 10% VEC electrolyte has a higher relative content of polycarbonate species.
- (2) The SEI film formed in 10% VEC electrolyte contains a greater amount of decomposition products of LiPF_6 ($\text{Li}_x\text{PO}_y\text{F}_z$ and LiF), in which the LiF component is predominant.

From the differences of SEI layers formed in the two electrolytes, it is assumed that the morphology of Li deposition on the substrate be also different. To prove this assumption, SEM images after 10 cycles were performed (Figure 4). As shown in Figure 4a,b, the interface of Li-metal anode and electrolyte without VEC exhibits an uneven and porous morphology with massive cracks. Extensive Li dendrites with a needlelike structure are clearly observable due to the poor protection effect of unsatisfactory SEI layer (even only after the initial Li deposition process, a large amount of Li dendrites are also formed (Figure S4)). In sharp contrast, the surface is smooth and homogeneous in the electrolyte with VEC, and no obvious Li dendrites and cracks are observed (Figures 4c,d and S5).

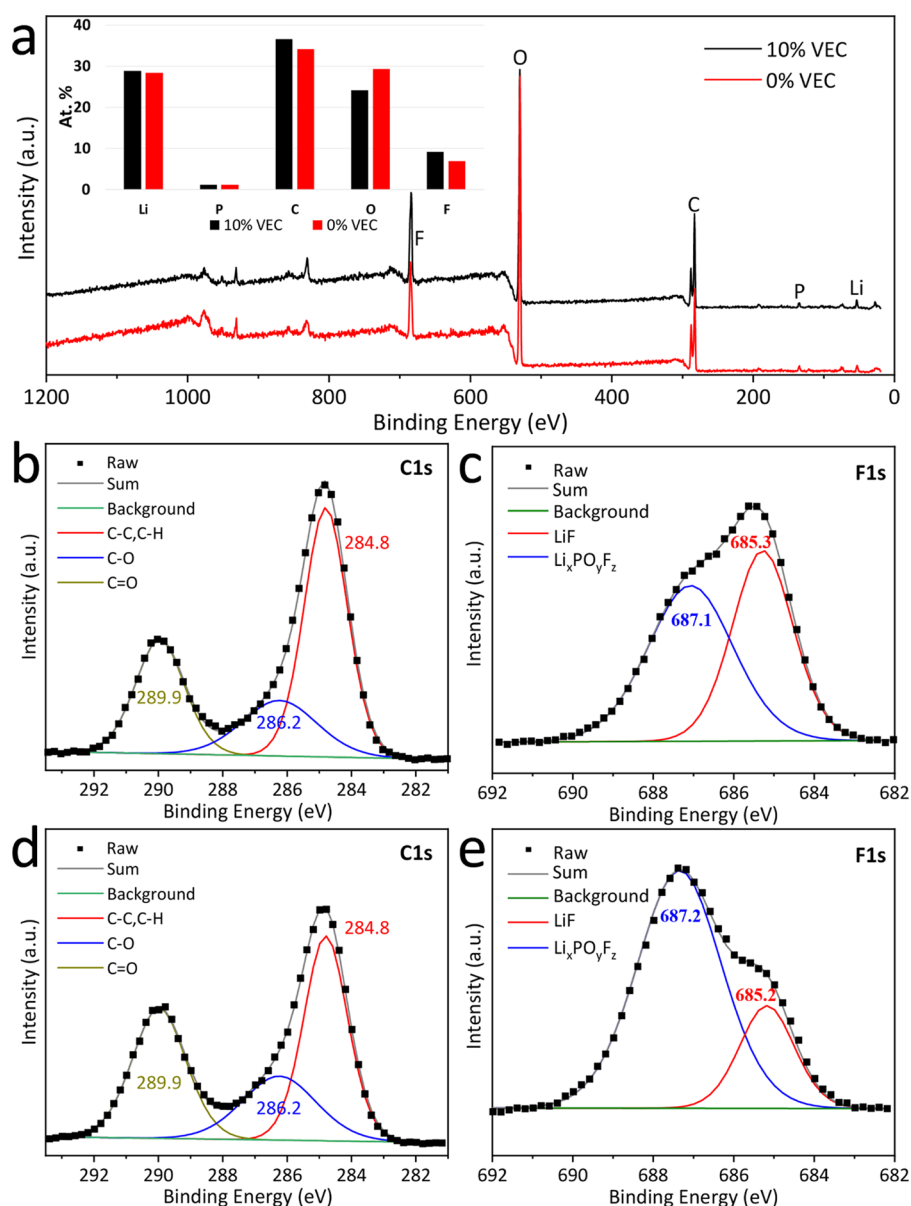


Figure 3. XPS characterization of SEI films formed on the Cu foil electrodes after 10 cycles at 0.25 mA cm^{-2} for 1.0 mAh cm^{-2} in different electrolytes. (a) XPS images (the inset table shows the atomic ratio of elements). (b, c) 1 M LiPF_6 in EC/DEC (1:1 by volume) with 10% VEC and (d, e) 1 M LiPF_6 in EC/DEC (1:1 by volume) without VEC.

To better understand the effects of different SEI interfaces on Li deposition, we simulated the deposition behavior of Li metal in both of the above electrodes by using COMSOL Multiphysics software. The red frame regions in the SEM images (Figure S6a,c; area, $5 \mu\text{m} \times 5 \mu\text{m}$) were used for the acquisition of grayscale information. And the obtained grayscale information can be further translated into altitude information to construct the studied three-dimensional (3D) models (Figure S6b,e) in COMSOL software finally. Several holes are clearly visible on the interface of Li-metal anode and electrolyte without VEC. Accordingly, the Li^+ -ion flux near these holes is enhanced dramatically (Figure 5a), which can be seen as hotspots for Li deposition. Consequently, the deposition rate of Li metal in the hotspots is much higher, which causes the nonuniform deposition process and the formation of pillarlike Li whisker (Figure 5b and Video S1). In sharp contrast, the electrode surface is relatively smooth in the electrolyte with 10% VEC added. And homogeneous Li^+ ion

flux near the interface (Figure 5c) can lead to uniform Li deposition behavior (Figure 5d and Video S2). The 3D morphology evolution of both electrodes was also simulated (Figure 6). Obviously, the relative height change in the electrolyte with 10% VEC (Figure 6c,d and Video S4) is much milder than that in the electrolyte without VEC (Figure 6a,b and Video S3).

The cycling performances of Li–Cu cells in 10% VEC and VEC-free electrolytes at the current density of 0.25 mA cm^{-2} with the cycling capacity of 1 mAh cm^{-2} had been investigated (Figure 7). The CE of Li–Cu cell in the VEC-free electrolyte exhibited an obvious and gradual decrease and dropped below 80% after 50 cycles. Moreover, an obvious short-circuit phenomenon (short circuit can be observed from abrupt CE increases or drops) appeared after ~ 80 cycles due to uncontrollable growth of Li dendrites and remarkable accumulation of dead Li during cycling. However, the CE of Li–Cu cell in the 10% VEC electrolyte was retained above 93.2% after 100 cycles, and no short circuit was observed. After 100 cycles at the higher

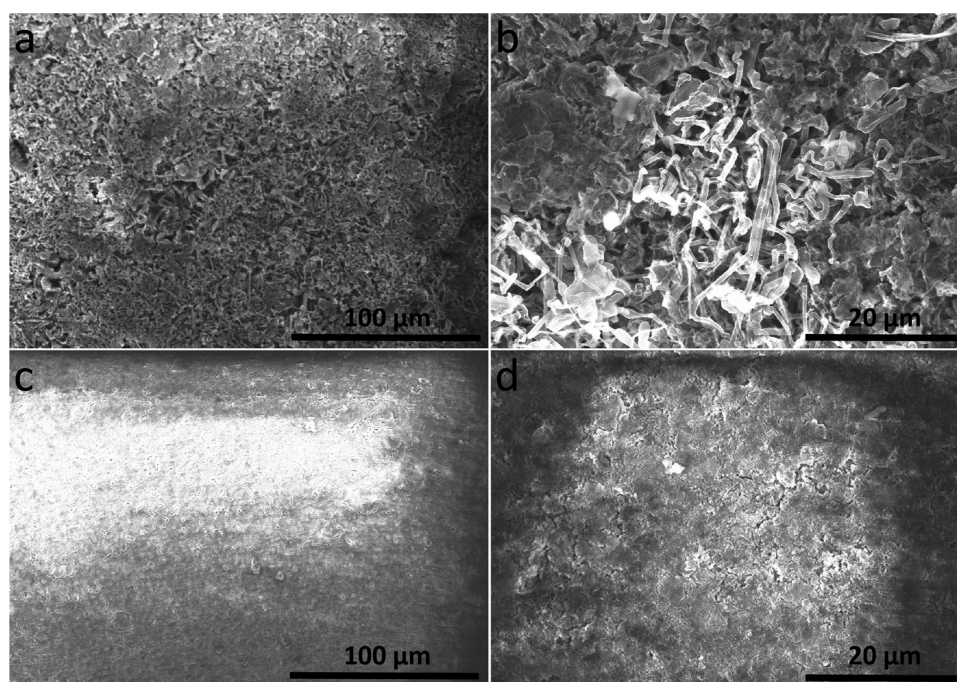


Figure 4. SEM images of the Cu foil electrodes at Li deposition state after 10 cycles of galvanostatic stripping/plating at 0.25 mA cm^{-2} for 1.0 mAh cm^{-2} in different electrolytes: (a, b) 1 M LiPF_6 in EC/DEC (1:1 by volume) without VEC and (c, d) 1 M LiPF_6 in EC/DEC (1:1 by volume) with 10% VEC.

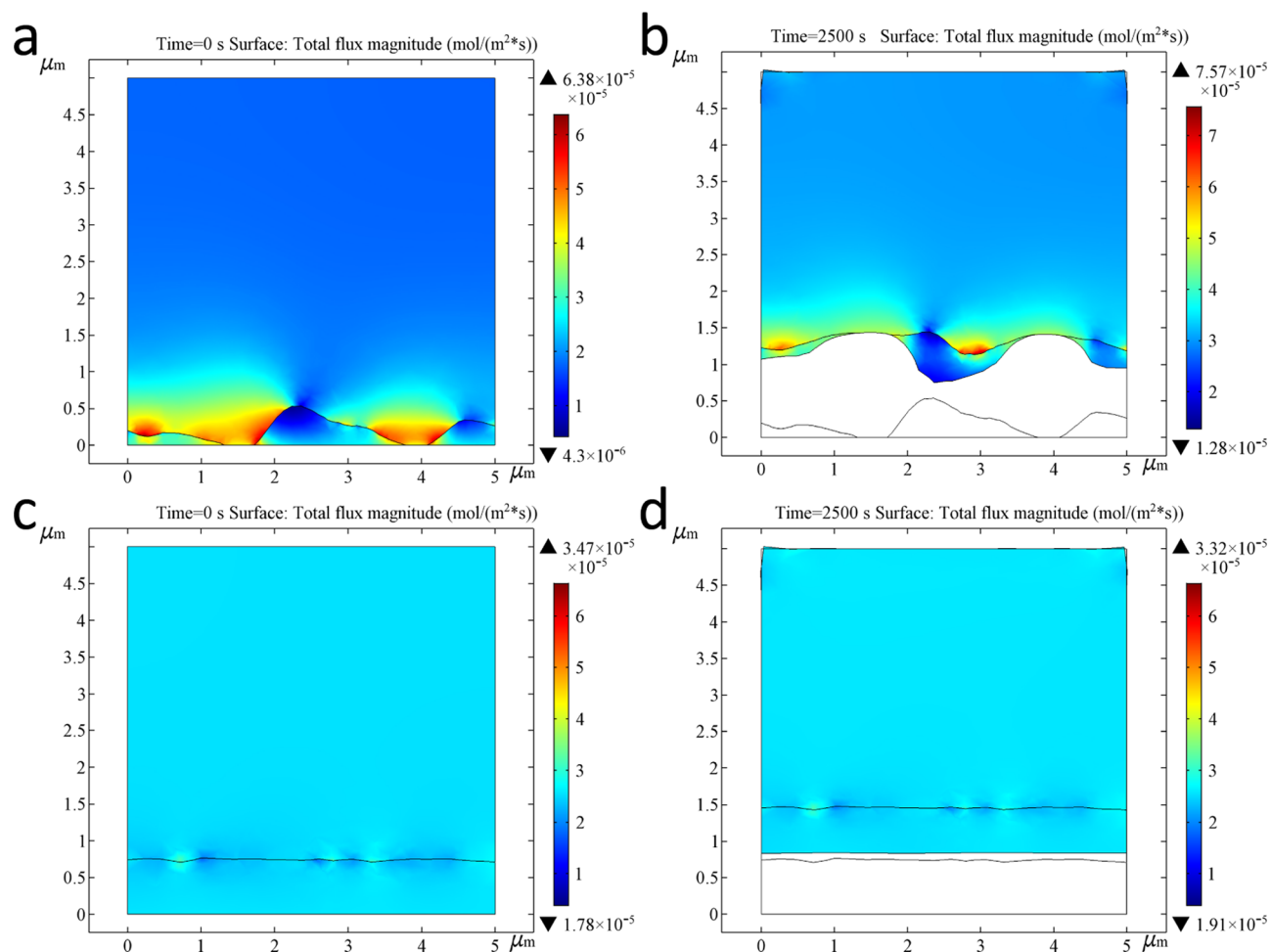


Figure 5. Simulations of the Cu foil electrode in the cross-sectional view with 1 M LiPF_6 in EC/DEC (1:1 by volume) as the electrolyte (a) at the pristine state and (b) after 2500 s Li deposition at 0.25 mA cm^{-2} . Simulations of the Cu foil electrode in the cross-sectional view with 1 M LiPF_6 in EC/DEC (1:1 by volume) and 10% VEC as the electrolyte (c) at the pristine state and (d) after 2500 s Li deposition at 0.25 mA cm^{-2} .

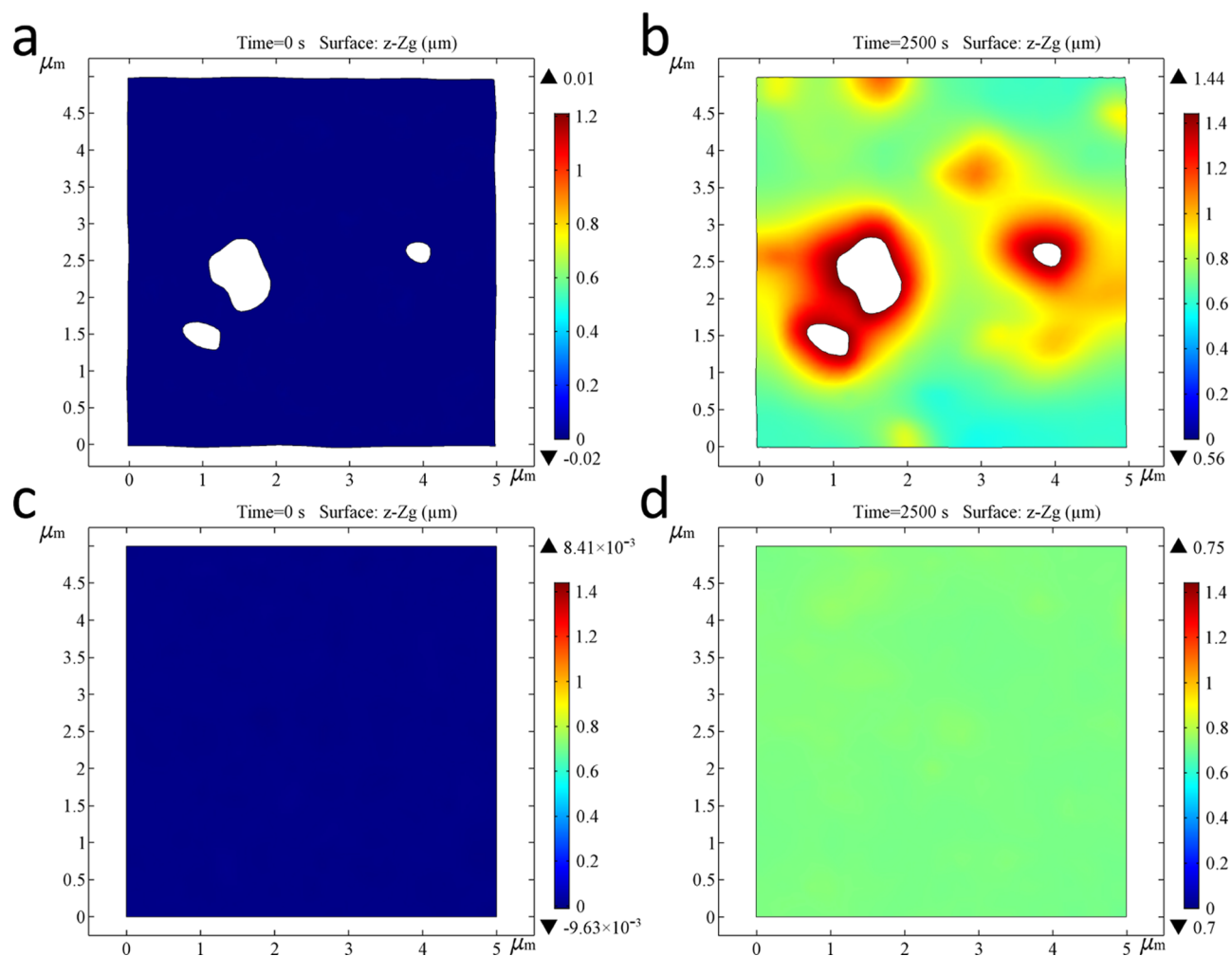


Figure 6. Relative height change of electrodes at the pristine state with different electrolytes: (a) 1 M LiPF₆ in EC/DEC (1:1 by volume) without VEC and (c) 1 M LiPF₆ in EC/DEC (1:1 by volume) with 10% VEC. The relative height change of electrodes after 2500 s Li deposition at 0.25 mA cm⁻² with (b) 1 M LiPF₆ in EC/DEC (1:1 by volume) without VEC and (d) 1 M LiPF₆ in EC/DEC (1:1 by volume) with 10% VEC.

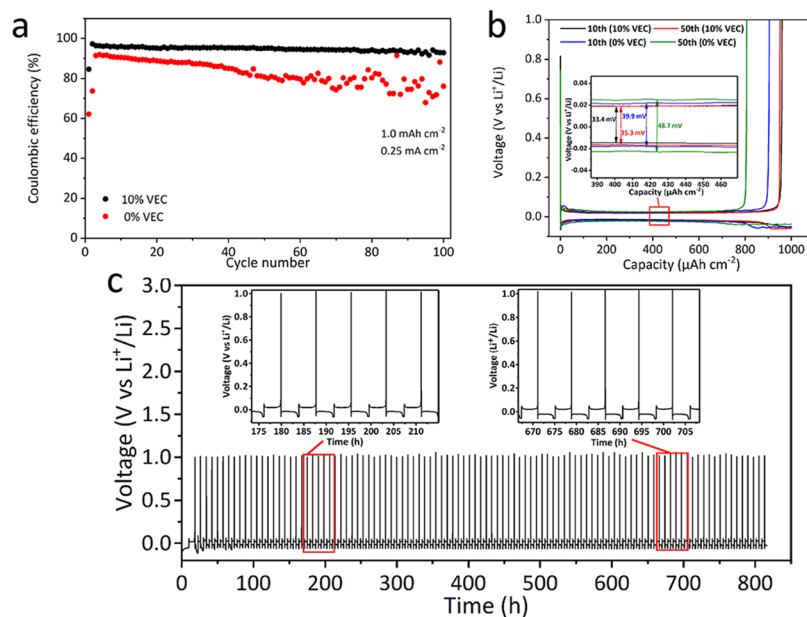


Figure 7. (a) Coulombic efficiency (CE) and (b) typical voltage profiles of Li–Cu cells in 10% VEC and VEC-free electrolytes at 0.25 mA cm⁻² with a cycling capacity of 1 mAh cm⁻². (c) Voltage stability of the Li–Cu cell at 0.25 mA cm⁻² for 1 mAh cm⁻².

current density of 0.5 and 1.0 mA cm⁻², the Li–Cu cells in the 10% VEC electrolyte still maintain high CEs of 93.4 and 94.0%, respectively (Figure S7). The improved cycling performance in 10% VEC electrolyte was further corroborated by the galvanostatic charge–discharge voltage profiles (Figure 7b). Polarization voltage of Li–Cu cell in 10% VEC electrolyte only rose slightly from 33.4 mV (10th cycle) to 35.3 mV (50th cycle). Moreover, the cell voltage was rather stable without obvious fluctuation during a relatively long cycling life span of 816 h (Figure 7c). In contrast, the increase in polarization voltage was much more prominent (from 39.9 to 48.7 mV after 40 cycles) for the Li–Cu cell in VEC-free electrolyte, which originates from the unstable SEI layer. The electrochemical performance of the Li-deposited CuLiFePO₄ full cell in 10% VEC electrolyte was also investigated (Figure S8).

EIS tests were conducted to further reveal the electrochemical characteristics of Cu foil electrodes in both the electrolytes (Figure S9). And the inset equivalent circuit is employed for the simulation of Nyquist plots. R_{sei} and R_{ct} are considered to be the SEI film resistance and charge-transfer resistance, respectively.⁴⁴ Clearly, the SEI film resistance (13.11 Ω) and charge-transfer resistance (58.34 Ω) of the Cu foil electrode after 20 cycles in 10% VEC electrolyte are lower than those in VEC-free electrolyte (27.19 and 72.88 Ω, respectively), confirming an enhanced charge-transfer process. As the Li deposition/stripping processes continue, the R_{sei} and R_{ct} values of the Cu foil electrode after 50 cycles in VEC-free electrolyte dramatically increased to 160.6 and 874.0 Ω, respectively, because of the continuous accumulation of high-resistance dead Li. However, the increments in the R_{sei} and R_{ct} values after 50 cycles (49.66 and 139.6 Ω, respectively) in 10% VEC electrolyte are greatly reduced, indicating that the formation of dead Li is effectively restrained by the well-established SEI layer in 10% VEC electrolyte.

4. CONCLUSIONS

In summary, positive effects of VEC as an additive for Li-metal anodes in carbonate-based electrolyte were identified. The DFT calculation results indicate that VEC decreased predominantly on Li-metal anodes at low potentials owing to its very low LUMO energy level (−0.82 eV). And the SEI film formed in 10% VEC electrolyte contains a higher relative content of polycarbonate species and a greater amount of decomposition products of LiPF₆ salt. Thus, the presence of VEC is beneficial to form a stable and smooth SEI layer, which can effectively suppress the growth of Li dendrites and reduce the side reactions between Li-metal electrode and the electrolyte. As a result, the Li–Cu cell exhibits a long life span of 816 h (100 cycles) with a high Coulombic efficiency of 93.2% at 0.25 mA cm⁻² with a specific areal capacity of 1.0 mAh cm⁻².

■ ASSOCIATED CONTENT

Supporting Information

The Supporting Information is available free of charge on the ACS Publications website at DOI: 10.1021/acsami.8b20706.

Time–current profiles of the Li–Cu cell at 0 V (vs Li⁺/Li) in 0% VEC and 10% VEC electrolytes; possible reduction products of DEC, EC, and VEC; XPS characterization of SEI films formed on the Cu foil electrodes after 25 cycles at 0.25 mA cm⁻² for 1.0 mAh cm⁻² in 10% VEC electrolyte; SEM images of the Cu foil electrode after the initial Li deposition in VEC-free electrolyte; SEM

images of the Cu foil electrodes at Li deposition state after galvanostatic stripping/plating after 10 cycles in 10% VEC electrolyte with higher magnification; COMSOL simulation models constructed by converting grayscale information to altitude; the CE of Li–Cu cells in 10% VEC and VEC-free electrolytes at higher current densities; cycling performance of Cu–Li/LiFePO₄ full cell in 10% VEC electrolyte; electrochemical impedance spectra of the Cu foil electrodes in 10% VEC and VEC-free electrolytes (PDF)

Nonuniform deposition process and the formation of pillarlike Li whisker (AVI)

Uniform Li deposition behavior (AVI)

Height change in the electrolyte without VEC (AVI)

Height change in the electrolyte with VEC (AVI)

■ AUTHOR INFORMATION

Corresponding Authors

*E-mail: licc@gdut.edu.cn (C.L.).

*E-mail: jbzhaoy@xmu.edu.cn (J.Z.).

ORCID

Chengchao Li: 0000-0003-2434-760X

Jinbao Zhao: 0000-0002-2753-7508

Notes

The authors declare no competing financial interest.

■ ACKNOWLEDGMENTS

This work was partially supported by the National Natural Science Foundation of China (21321062).

■ REFERENCES

- (1) Etacheri, V.; Marom, R.; Elazari, R.; Salitra, G.; Aurbach, D. Challenges in the Development of Advanced Li-Ion Batteries: a review. *Energy Environ. Sci.* **2011**, *4*, 3243–3262.
- (2) Tarascon, J. M.; Armand, M. Issues and Challenges Facing Rechargeable Lithium Batteries. *Nature* **2001**, *414*, 359–367.
- (3) Xiang, H. F.; Jin, Q. Y.; Chen, C. H.; Ge, X. W.; Guo, S.; Sun, J. H. Dimethyl Methylphosphonate-Based Nonflammable Electrolyte and High Safety Lithium-Ion Batteries. *J. Power Sources* **2007**, *174*, 335–341.
- (4) Li, Q.; Zhu, S.; Lu, Y. 3D Porous Cu Current Collector/Li-Metal Composite Anode for Stable Lithium-Metal Batteries. *Adv. Funct. Mater.* **2017**, *27*, No. 1606422.
- (5) Lin, D.; Zhao, J.; Sun, J.; Yao, H.; Liu, Y.; Yan, K.; Cui, Y. Three-Dimensional Stable Lithium Metal Anode with Nanoscale Lithium Islands Embedded in Ionically Conductive Solid Matrix. *Proc. Natl. Acad. Sci. U.S.A.* **2017**, *114*, 4613–4618.
- (6) Cheng, X.-B.; Hou, T.-Z.; Zhang, R.; Peng, H.-J.; Zhao, C.-Z.; Huang, J.-Q.; Zhang, Q. Dendrite-Free Lithium Deposition Induced by Uniformly Distributed Lithium Ions for Efficient Lithium Metal Batteries. *Adv. Mater.* **2016**, *28*, 2888–2895.
- (7) Schipper, F.; Aurbach, D. A Brief Review: Past, Present and Future of Lithium Ion Batteries. *Russ. J. Electrochem.* **2016**, *52*, 1095–1121.
- (8) Whittingham, M. S. Chemistry of Intercalation Compounds: Metal Guests in Chalcogenide Hosts. *Prog. Solid State Chem.* **1978**, *12*, 41–99.
- (9) Li, N.-W.; Ya-Xia, Y.; Chun-Peng, Y.; Yu-Guo, G. An Artificial Solid Electrolyte Interphase Layer for Stable Lithium Metal Anodes. *Adv. Mater.* **2016**, *28*, 1853–1858.
- (10) Zheng, G. Y.; Wang, C.; Pei, A.; Lopez, J.; Shi, F. F.; Chen, Z.; Sendek, A. D.; Lee, H. W.; Lu, Z. D.; Schneider, H.; Safont-Sempere, M. M.; Chu, S.; Bao, Z. N.; Cui, Y. High-Performance Lithium Metal Negative Electrode with a Soft and Flowable Polymer Coating. *ACS Energy Lett.* **2016**, *1*, 1247–1255.

- (11) Zhu, B.; Jin, Y.; Hu, X.; Zheng, Q.; Zhang, S.; Wang, Q.; Zhu, J. Poly(dimethylsiloxane) Thin Film as a Stable Interfacial Layer for High-Performance Lithium-Metal Battery Anodes. *Adv. Mater.* **2017**, *29*, No. 1603755.
- (12) Hu, Z.; Zhang, S.; Dong, S.; Li, W.; Li, H.; Cui, G.; Chen, L. Poly(ethyl α -cyanoacrylate)-Based Artificial Solid Electrolyte Interphase Layer for Enhanced Interface Stability of Li Metal Anodes. *Chem. Mater.* **2017**, *29*, 4682–4689.
- (13) Fan, L.; Zhuang, H. L. L.; Gao, L. N.; Lu, Y. Y.; Archer, L. A. Regulating Li Deposition at Artificial Solid Electrolyte Interphases. *J. Mater. Chem. A* **2017**, *5*, 3483–3492.
- (14) Xu, R.; Zhang, X. Q.; Cheng, X. B.; Peng, H. J.; Zhao, C. Z.; Yan, C.; Huang, J. Q. Artificial Soft-Rigid Protective Layer for Dendrite-Free Lithium Metal Anode. *Adv. Funct. Mater.* **2018**, *28*, No. 1705838.
- (15) Shi, P.; Zhang, L.; Xiang, H.; Liang, X.; Sun, Y.; Xu, W. Lithium Difluorophosphate as a Dendrite-Suppressing Additive for Lithium Metal Batteries. *ACS Appl. Mater. Interfaces* **2018**, *10*, 22201–22209.
- (16) Zheng, H.; Xie, Y.; Xiang, H.; Shi, P.; Liang, X.; Xu, W. A Bifunctional Electrolyte Additive for Separator Wetting and Dendrite Suppression in Lithium Metal Batteries. *Electrochim. Acta* **2018**, *270*, 62–69.
- (17) Shi, P.; Zheng, H.; Liang, X.; Sun, Y.; Cheng, S.; Chen, C.; Xiang, H. A Highly Concentrated Phosphate-Based Electrolyte for High-Safety Rechargeable Lithium Batteries. *Chem. Commun.* **2018**, *54*, 4453–4456.
- (18) Xu, K. Nonaqueous Liquid Electrolytes for Lithium-Based Rechargeable Batteries. *Chem. Rev.* **2004**, *104*, 4303–4418.
- (19) Xu, K. Electrolytes and Interphases in Li-Ion Batteries and Beyond. *Chem. Rev.* **2014**, *114*, 11503–11618.
- (20) Xiong, S.; Xie, K.; Diao, Y.; Hong, X. Characterization of the Solid Electrolyte Interphase on Lithium Anode for Preventing the Shuttle Mechanism in Lithium–Sulfur Batteries. *J. Power Sources* **2014**, *246*, 840–845.
- (21) Cheng, X.-B.; Yan, C.; Chen, X.; Guan, C.; Huang, J.-Q.; Peng, H.-J.; Zhang, R.; Yang, S.-T.; Zhang, Q. Implantable Solid Electrolyte Interphase in Lithium-Metal Batteries. *Chem* **2017**, *2*, 258–270.
- (22) Jia, W.; Fan, C.; Wang, L.; Wang, Q.; Zhao, M.; Zhou, A.; Li, J. Extremely Accessible Potassium Nitrate (KNO₃) as the Highly Efficient Electrolyte Additive in Lithium Battery. *ACS Appl. Mater. Interfaces* **2016**, *8*, 15399–15405.
- (23) Miao, R.; Yang, J.; Xu, Z.; Wang, J.; Nuli, Y.; Sun, L. A New Ether-Based Electrolyte for Dendrite-Free Lithium-Metal Based Rechargeable Batteries. *Sci. Rep.* **2016**, *6*, No. 21771.
- (24) Sano, H.; Sakaebe, H.; Matsumoto, H. Observation of Electrodeposited Lithium by Optical Microscope in Room Temperature Ionic Liquid-Based Electrolyte. *J. Power Sources* **2011**, *196*, 6663–6669.
- (25) Zhang, X.-Q.; Cheng, X.-B.; Chen, X.; Yan, C.; Zhang, Q. Fluoroethylene Carbonate Additives to Render Uniform Li Deposits in Lithium Metal Batteries. *Adv. Funct. Mater.* **2017**, *27*, No. 1605989.
- (26) Markevich, E.; Salitra, G.; Chesneau, F.; Schmidt, M.; Aurbach, D. Very Stable Lithium Metal Stripping–Plating at a High Rate and High Areal Capacity in Fluoroethylene Carbonate-Based Organic Electrolyte Solution. *ACS Energy Lett.* **2017**, *2*, 1321–1326.
- (27) Newman, M. S.; Addor, R. W. Synthesis and Reactions of Vinylene Carbonate. *J. Am. Chem. Soc.* **1955**, *77*, 3789–3793.
- (28) Hu, Y.; Kong, W.; Li, H.; Huang, X.; Chen, L. Experimental and Theoretical Studies on Reduction Mechanism of Vinyl Ethylene Carbonate on Graphite Anode for Lithium Ion Batteries. *Electrochim. Commun.* **2004**, *6*, 126–131.
- (29) Ma, L.; Xia, J.; Xia, X.; Dahn, J. R. The Impact of Vinylene Carbonate, Fluoroethylene Carbonate and Vinyl Ethylene Carbonate Electrolyte Additives on Electrode/Electrolyte Reactivity Studied Using Accelerating Rate Calorimetry. *J. Electrochem. Soc.* **2014**, *161*, A1495–A1498.
- (30) Nam, T.-H.; Shim, E.-G.; Kim, J.-G.; Kim, H.-S.; Moon, S.-I. Electrochemical Performance of Li-Ion Batteries Containing Biphenyl Vinyl Ethylene Carbonate in Liquid Electrolyte. *J. Electrochem. Soc.* **2007**, *154*, A957–A963.
- (31) Xiang, H.; Chen, J.; Wang, H. Effect of Vinyl Ethylene Carbonate on the Compatibility Between Graphite and the Flame-Retarded Electrolytes Containing Dimethyl Methyl Phosphonate. *Ionics* **2011**, *17*, 415–420.
- (32) Xu, S. D.; Zhuang, Q. C.; Wang, J.; Xu, Y. Q.; Zhu, Y. B. New Insight into Vinylene Carbonate as a Film Forming Additive to Ethylene Carbonate-Based Electrolytes for Lithium-Ion Batteries. *Int. J. Electrochem. Sci.* **2013**, *8*, 8058–8076.
- (33) Zhou, R.; Huang, J.; Lai, S.; Li, J.; Wang, F.; Chen, Z.; Lin, W.; Li, C.; Wang, J.; Zhao, J. A Bifunctional Electrolyte Additive for H₂O/HF Scavenging and Enhanced Graphite/LiNi_{0.5}Co_{0.2}Mn_{0.3}O₂ Cell Performance at a High Voltage. *Sustainable Energy Fuels* **2018**, *2*, 1481–1490.
- (34) Aurbach, D.; Gamolsky, K.; Markovsky, B.; Gofer, Y.; Schmidt, M.; Heider, U. On the Use of Vinylene Carbonate (VC) as an Additive to Electrolyte Solutions for Li-Ion Batteries. *Electrochim. Acta* **2002**, *47*, 1423–1439.
- (35) Aurbach, D.; Ein-Ely, Y.; Zaban, A. The Surface Chemistry of Lithium Electrodes in Alkyl Carbonate Solutions. *J. Electrochem. Soc.* **1994**, *141*, L1–L3.
- (36) Chen, L. B.; Wang, K.; Xie, X. H.; Xie, J. Y. Effect of Vinylene Carbonate (VC) as Electrolyte Additive on Electrochemical Performance of Si Film Anode for Lithium Ion Batteries. *J. Power Sources* **2007**, *174*, S38–S43.
- (37) Vogl, U. S.; Lux, S. F.; Crumlin, E. J.; Liu, Z.; Terborg, L.; Winter, M.; Kostecki, R. The Mechanism of SEI Formation on a Single Crystal Si(100) Electrode. *J. Electrochem. Soc.* **2015**, *162*, A603–A607.
- (38) Zaban, A.; Aurbach, D. Impedance Spectroscopy of Lithium and Nickel Electrodes in Propylene Carbonate Solutions of Different Lithium Salts a Comparative Study. *J. Power Sources* **1995**, *54*, 289–295.
- (39) Etacheri, V.; Haik, O.; Goffer, Y.; Roberts, G. A.; Stefan, I. C.; Fasching, R.; Aurbach, D. Effect of Fluoroethylene Carbonate (FEC) on the Performance and Surface Chemistry of Si-Nanowire Li-Ion Battery Anodes. *Langmuir* **2012**, *28*, 965–976.
- (40) Zhu, J.; Yang, J.; Zhou, J.; Zhang, T.; Li, L.; Wang, J.; Nuli, Y. A Stable Organic-Inorganic Hybrid Layer Protected Lithium Metal Anode for Long-Cycle Lithium-Oxygen Batteries. *J. Power Sources* **2017**, *366*, 265–269.
- (41) Liu, Q. C.; Xu, J. J.; Yuan, S.; Chang, Z. W.; Xu, D.; Yin, Y. B.; Li, L.; Zhong, H. X.; Jiang, Y. S.; Yan, J. M.; Zhang, X. B. Artificial Protection Film on Lithium Metal Anode toward Long-Cycle-Life Lithium-Oxygen Batteries. *Adv. Mater.* **2015**, *27*, S241–S247.
- (42) Lu, Y.; Tu, Z. Y.; Archer, L. A. Stable Lithium Electrodeposition in Liquid and Nanoporous Solid Electrolytes. *Nat. Mater.* **2014**, *13*, 961–969.
- (43) Pan, J.; Cheng, Y. T.; Qi, Y. General Method to Predict Voltage-Dependent Ionic Conduction in a Solid Electrolyte Coating on Electrodes. *Phys. Rev. B* **2015**, *91*, No. 134116.
- (44) Lee, H.; Song, J.; Kim, Y.-J.; Park, J.-K.; Kim, H.-T. Structural Modulation of Lithium Metal-Electrolyte Interface with Three-Dimensional Metallic Interlayer for High-Performance Lithium Metal Batteries. *Sci. Rep.* **2016**, *6*, No. 30830.